Technology Performance Report

(Phase One)

Smart Grid Demonstration Program

Contract ID: DE-OE0000232

Sub-Area: 2.5 Demonstration of Promising Energy Storage Technologies

Project Type: Flywheel Energy Storage Demonstration

Revision: V2.1

Company Name: Amber Kinetics, Inc.

April 16, 2012

ACKNOWLEDGMENT:

This material is based upon work supported by the Department of Energy under Award Number(s) DE-OE0000232.

DISCLAIMER:

TABLE OF CONTENTS

1. Overview of the Energy Storage Project

This project aims to develop and demonstrate significantly improved, lower-cost flywheel energy storage technology for energy storage applications. Phase 1 & 2 of the project intends to focus on the development of advanced flywheel energy storage technology with the following key initiatives: reduce flywheel rotor cost (>10x), improve round-trip energy storage efficiency, and integrate lower-cost magnetic bearings with minimal energy losses. Phase 1 & 2 will focus on the research & development of Amber Kinetics' new technology. A grid-connected demonstration is not anticipated in the first two phases of this program.

Table 1- Project Objectives by Phase

Phase	Project Objective
One	Prototype Flywheel (Engineering Scale)
Two	Prototype Flywheel (Commercial Scale)
Three	Flywheel Demonstration (Grid Connected)

Phase 1:

The objective of Phase 1 is to demonstrate an engineering-scale prototype flywheel energy storage system suitable for data measurements and performance monitoring. The prototype flywheel stores approximately 5 kWh of energy. The following tests are conducted in a controlled laboratory environment. The prototype flywheel system is connected to a 300V DC bus supplying electrical energy into the system's power control electronics:

Test 1: Spin up flywheel system from rest to maximum design speed for 5 kWh of storage. Measure RPM with sensors connected to Lab View software to output data in real-time. Monitor for any imbalance or rotor-dynamic instabilities preventing flywheel system from reaching maximum design speed.

Validation: Balance and rotor-dynamic stability of the flywheel rotor throughout the entire operating range of the flywheel.

Test 2: Spin up flywheel system to maximum speed, and perform coasting test for a period of 24 hours (introducing no load causing discharge). Measure magnetic bearing and power electronics power draw during 24-hour period to develop baseline for system ancillary power requirements using Lab view sensors with data output into Lab view software for analysis. Measure flywheel RPM at the end of 24 hours to determine total coasting losses (air drag + eddy current losses).

Validation: Idling losses on the order of less than 0.5% from air drag, eddy currents, and power electronics.

Test 3: Spin up flywheel system to maximum speed, let coast for period of 24 hours, then discharge flywheel completely to rest. Measure total amount of energy withdrawn from flywheel system to determine round-trip storage efficiency to 300V DC bus. Measure amount of power required in magnetic bearing system to maintain axial stability in the flywheel (power requirement amounts to losses) using Lab view equipment.

Validation: High round-trip efficiency (80%+)

Key technical milestones will be discussed in Technology Progress Reports submitted periodically to the Amber Kinetics Project Officer.

These tests will primarily serve as a baseline used to compare the results of further testing under different operating conditions (heavy duty cycles, increased / reduced temperatures, performance from 40-80% of maximum design speed, etc.). Measurements of flywheel performance as a function of increased temperature within the vacuum vessel will also be performed and recorded. Testing of the prototype system will be performed over a period of several months with a final test report with complete findings delivered to DOE immediately thereafter.

2. Description of Energy Storage Technologies & Systems

The Amber Kinetics program is developing and demonstrating lower cost flywheel energy storage technology. A flywheel stores energy by taking electrical energy and converting it into rotational kinetic energy. The kinetic energy is stored in a rotor spinning at high speeds and levitated by electromagnetic bearings to minimize friction and reduce drag losses. To retrieve the energy, the flywheel motor-generator slows down the flywheel rotor and converts the kinetic energy back into electricity.

3. Description of the Analysis Methodologies

3.1 Flywheel Data Acquisition

The Amber Kinetics Gen1 flywheel is monitored using a National Instruments Labview data acquisition system. The flywheel is completely instrumented to measure both electrical and mechanical parameters.

A National Instruments Labview station is used to display and log all flywheel information. A single computer is outfitted with a high-speed Labview DAQ card capable of acquiring data at 50kHz. A remote National Instruments SCXI 1000 chassis contains two conditioning cards (NI 1102 and NI1120) for acquiring and filtering analog inputs. Analog inputs include current sensors, voltage sensors, position sensors, RTD and infrared temperature sensors, and vacuum.

Some information is brought in directly from the motor drive, supervisory and magnetic bearing controllers. These controllers broadcast their data via CAN bus; the CAN bus data

reaches a CAN-USB interface where it can also be directed to LABVIEW for display and logging.

The Labview DAQ card samples data at a relatively high speed of 50 kHz and then reduces the data to a single value that is typically logged at a period of 1.0 to 2.5 sec. Depending on the sensor, some values are averages of many samples. System DC voltage and current are an average of a large number of points. Flywheel terminal power is computed by performing instantaneous products of currents and voltages and then averaging the result. Other quantities such as temperature and vacuum are simple averages of a small number of values. Quantities that are preprocessed inside micro-controllers are sampled at 40kHz, digitally filtered and reduced to a single value for Labview.

Table 2 - Labview DAQ Hardware

National Instruments Equipment	**Model**
PC High-speed DAQ Card	NI 6035E
Remote DAQ Chassis	SCXI 1000
32-Ch Analog Card	NI1102
Termination Module for NI1102	NI 1303
8-Ch Isolated Input	NI1120
Termination Module for NI1120	NI 1327

3.2 System Instrumentation

Please refer to Figure 1 and Table 1 below for the following discussion:

Figure 1 – Prototype Flywheel System Architecture

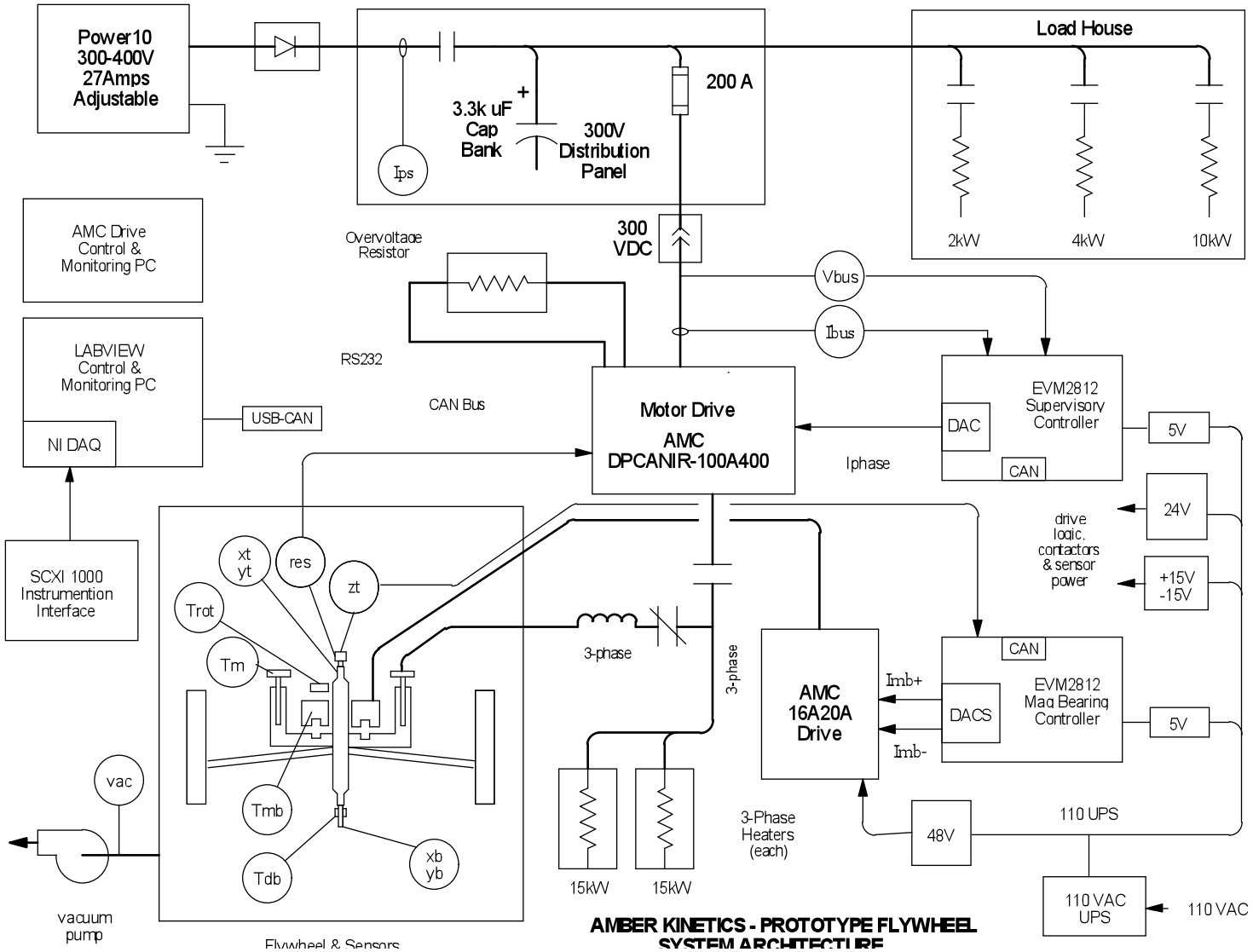

Label	Transducers	Sensor Model	Accuracy	Installed Range	Signal Type	Conditioner	Filter	Samp. Rate	LabV Samp.	Labview Processing	CAN	CAN Rate
Tmb	Temperature Mag Bearing Stator	Omega 100 ohm RTD	± 4 F	0 to 200 F	0-20ma	Omega CN491A, NI 1102	1 Hz	50kHz	100	Average		
Tmot	Temperature Motor Stator	Omega 100 ohm RTD	± 4 F	0 to 200 F	0-20ma	Omega CN491A	1 Hz	50kHz	100	Average		
Trb	Temperature Radial Bearing	Omega 100 ohm RTD	± 4 F	0 to 200 F	0-20ma	Omega CN491A	1 Hz	50kHz	100	Average		
Trot	Infrared Temperature Flywheel Rotor	Exergen IRt/c.1x	± 4 F	0 to 150 F	0-20ma	0 to 20ma converter	none	50kHz	100	Average		
Pvac	Vacuum Pressure Sensor	Moducell 325	5 mTorr	0 to 10000 mTorr	0-10V	NI 1102 Card	1 Hz	50kHz	100	Average		
Vbus	Flywheel Bus Voltage Sensor (to SPV MCU)	LEM LV25P	± 3.6V	450V	±20ma	R/C filter	1kHz	40kHz			x	10Hz
Ibus_pos	Flywheel Bus Current Pos (to SPV MCU)	LEM LF306S	± 0.2A	45A	±20ma	R/C filter	1kHz	40kHz			x	10Hz
Ibus_neg	Flywheel Bus Current Neg (to SPV MCU)	LEM LF306S	± 0.2A	-45A	±20ma	R/C filter	1kHz	40kHz			x	10Hz
Ips	Power Supply Current at Wall	LEM LT500S	± 2.5A	500A	±20ma	NI 1120 Card	4 kHz	50kHz		Average		
Va	Phase A phase voltage	LEM LV25P	± 2.5V	300V	±20ma	NI 1120 Card	4 kHz	50kHz	5000	3ph power calc.		
Vb	Phase B phase voltage	LEM LV25P	± 2.5V	300V	±20ma	NI 1120 Card	4 kHz	50kHz	5000	3ph power calc.		
Ia	Phase A phase current	Tektronix A621	± 0.5A	± 50A (0.1V/A)	±20ma	NI 1120 Card	4 kHz	50kHz	5000	3ph power calc.		
Ib	Phase B phase current	Tektronix A621	± 0.5A	± 50A (0.1V/A)	±20ma	NI 1120 Card	4 kHz	50kHz	5000	3ph power calc.		
Zt	Z-axis position sensor (to MB controller)	uEpsilon DT3010-S2-M	±0.001"	0 to .070"	0-14V	Mag Bearing MCU	none	40kHz	1	Log only	x	10Hz
Xt	X-top position sensor	uEpsilon DT3010-S1-M	±0.0005"	± 0.005"	0-14V	R/C filter	200Hz					
Yt	Y-top position sensor	uEpsilon DT3010-S1-M	±0.0005"	± 0.005"	0-14V	R/C, NI 1120 Card	200Hz	50kHz	4000	p-p calc.		
Xb	X-bot position sensor	uEpsilon DT3010-S1-M	±0.0005"	± 0.010"	0-14V	R/C filter	200Hz					
Yb	Y-bot position sensor	uEpsilon DT3010-S1-M	±0.0005"	± 0.010"	0-14V	R/C filter, NI 1120 Card	200Hz	50kHz	4000	p-p calc.		
Res	Angle/Speed Resolver	RotaSyn RO5032	±0.2 deg	0 to 360 deg	sin/cos	AMC Drive	none				x	100Hz

	Computed Signals	**Computer**								
Imb	Mag Bearing command current	Mag bearing MCU	±0.25A	±15A	100Hz	n/a	1	Log only	x	10Hz
Zpos	Mag Bearing position	Mag bearing MCU	±0.001"	0 to .070"	100Hz	n/a	1	Log only	x	10Hz
Ibus	Ibus_pos - Ibus_net	Supervisory MCU	± 0.2A	±45A	100Hz	n/a	1	DC power calc.	x	10Hz
Vbus_filt	filtered Vbus	Supervisory MCU	± 3.6V	450V	100Hz	n/a	1	DC power calc.	x	10Hz

Table 3 – Input / Output List

3.3 Flywheel Sensors Description

Flywheel Speed and Position (RES)

A resolver type sensor (essentially a rotary transformer) will allow the angle and speed of the flywheel to be calculated. The absolute rotor angle is required for motor commutation and must be accurate to a few degrees. The speed can be easily calculated from this angle signal. The resolver is wired to the motor drive where the motor drive software conditions and scales the resolver to read both angular position and velocity. The velocity is broadcast over CAN so that it can be received and logged by the LABVIEW system.

Shaft Position Sensors (Xt, Yt, Zt, Xb, Yb)

A top x and y (lateral coordinates) and z (vertical axis) sensor is located near the top of the flywheel shaft; a bottom set is located near the bottom end. The z-sensor is sent to the magnetic bearing controller and then broadcast over CAN for logging and display. The x and y sensors are available as analog signals for display on an oscilloscope. The y-top and y-bottom sensors are also wired to LABVIEW for analysis and display of the machine runout.

All positions sensors are Eddy-current type probes made by uEpsilon. These probes are calibrated in place to ensure reliability and accuracy. The conditioning electronics is completely analog offering continuous resolution. Their accuracy is better than 0.001”.

Magnetic Bearing Temperature (Tmb)

An RTD is used to monitor the temperature of the top of the magnetic bearing stator core.

Motor Stator Temperature (Tmot)

An RTD is used to monitor the temperature of the motor stator. The sensor is mounted on a base plate that supports the stator. The actual wire temperature was found to be approx. 4-5 degF higher than that of the support plate in preliminary calibrations.

Rotor Surface Temperature (Trot)

An infrared thermal sensor monitors the surface temperature of the rotor shaft to verify that temperatures reach safe steady-state values during operation.

Lower Radial Stabilizer Bearing Temperature (Trb)

An RTD is used to monitor the temperature adjacent to the lower radial stabilizer.

Vacuum Pressure (Vac)

A vacuum sensor is used to monitor the vacuum pump to maintain the required vacuum (< 100 mTorr) in the flywheel containment.

3.4 Electrical Facility Measurements

Flywheel Bus Current and Voltage (Ibus, Vbus)

Flywheel voltage and current are monitored directly at the DC input to the AMC motor drive. Both voltage and current are measured using isolated Hall-effect current transformer sensors (LEM USA). The sensors are wired directly to the Supervisory micro-controller and then broadcast over CAN bus.

Flywheel system power is computed in LABVIEW as the product of current and voltage.

Power 300V Supply Current (Ips)

Main power supply current is measured using a LEM current sensor. This sensor is directly wired to the SCSI1000 chassis.

Load Current (Iload)

Load current is indirectly computed as the difference between the power supply current and the flywheel system current (Iload = Ips – Ibus). This calculation is performed by the Labview software.

Phase Voltages and Currents (Va, Vb, Ia, Ib)

Temporary voltage and current sensors are to be installed at the flywheel terminals (not shown in diagram) and brought into Labview at the SCSI 1000 chassis. Labview will make instantaneous high speed measurements of 3-phase power and then compute an average that can be used for accurate determination of the flywheel efficiency (apart from the power electronics). This flywheel terminal power can be compared with the flywheel system power to also estimate the motor drive efficiency.

3.5 Sensor Calibration

Calibration Standards

Calibration for each type of sensor is tracked to an accurate measurement source. The following sources are used:

Table 4 – Calibration Sources

Sensor	Calibration Instruments
Voltage	Agilent U1604A Handheld Digital Oscilloscope/Meter SN:KR49389001 Calibration Certificate: U1604AKR49389001 Oct. 4 2010
Current	Tektronix A622 Current Probe with Agilent U1604A 0 to 5A Accuracy verified with 5A, 50mV shunt
Position	Calibrated to 0.005" accuracy with BestTest dial indicator
Vacuum	Used Moducell Calibration Equation
Temperature	Tested in oven to 150 degF. Temperature verified with either WaveTek 28XT meter with thermocouple attachment, or EXTECH 42505 Handheld IR thermometer to ± 4 degF

Bus Voltage Calibration

The main DC bus was energized from the Power 10 power supply to 300 VDC as measured by the U1604A Digital Meter. The main bus sensor (Vbus) is wired to the Supervisory controller. The software offset was initially set to zero and the gain constant was then set to read out 300V on a CAN monitor screen as well as the Labview graph. Zero volts was rechecked and an offset was inserted if required. A few iterations were required to arrive at a repeatable calibration.

Calibration was rechecked at 250V and 350V with accuracy remaining within a few volts.

Bus Current Calibration

A current loop was temporarily wired from the Power 10 power supply through the main Bus Current sensors. In this system there is a separate sensor for positive current (Ibus_pos), and negative current (Ibus_neg); both these sensors are wired into the Supervisory controller similarly as for the Bus Voltage sensor (Vbus).

The initial software offsets were set to zero, and the software gains were precalculated for the LEM 306S sensors. A table of currents was created up to the full output of the power supply (~27A) for both positive and negative current senses. Values from the CAN monitor screen were logged and a linear curve fit was then performed between the measured and indicated currents. The curve fit coefficients were then used to recompute correct gains and offsets for the Supervisory controller constants. The final calibration was better than 0.5A accurate.

DC Power Accuracy

Based on the results for the Bus Current and Voltage calibrations. Power accuracies are estimated to be approximately ±150 Watts (0.5A * 300V).

Eddy-Probe Sensor Calibration

Eddy probes were calibrated over the expected ranges of motion of the flywheel shaft. Each sensor was independently calibrated in place by physically moving the shaft and monitoring its motion using a dial indicator.

The uEpsilon manual gives specific instructions on how to set the potentiometers in the conditioning electronics for each probe; this requires that 3 points be defined for setting of the pots. For each sensor, two extreme points, and one center point were defined.

The pots were first set to indicate voltages on the oscilloscope according to the following table:

Table 5 – Calibration

Sensors	Calibration Points	Corresponding Voltage
Ztop	0.070”, 0.040”, 0.010	0V, 4V, 8.0 Volts
Xtop, Ytop	-0.003”, 0”, 0.003”	1.0V, 2.5V, 4.0 Volts

Xbot, Ybot	-0.005”, 0, 0.005	1.0V, 2.5V, 4.0 Volts

Once the pots were set, then gain and offset constants were adjusted to read the appropriate values on the Labview and CAN monitor screens. Accuracies for the Ztop sensor were about ± 0.001 and accuracies for the X, Y sensors were within ±0.0002”.

4. Technology Performance Results

4.1 Overview

This section describes initial testing of Gen 1 rotor and flywheel system. Test articles comprise a dedicated spin test rotor and a complete prototype flywheel system (two rotors were manufactured in Phase 1). Testing included spin testing at a commercial spin test facility, characterization of the prototype, iterating prototype features to improve operability, performance testing, and loss measurements.

4.2 Test Protocol for Prototype Operation

General Procedures

The UUT (Unit Under Test) was mounted to the floor mounted using studs and leveling feet. The test engineer ensured all pre-test and safety procedures were observed including connecting and energizing the vacuum pump, establishing and verifying correct connection of all electrical wires and feeders, energizing the high voltage DC bus, energizing the 24 volt DC equipment, connecting the Data Acquisition System (DAQ) to the test article, and ensuring compliance with all safety procedures and precautions.

Test Execution

After initial settings were made for each test, the tests were executed manually by opening and closing contactors on the DC bus and sending explicit speed or current commands. The DAQ/LabVIEW collected data in text format, which was subsequently copied into spreadsheets for analysis.

4.3 Spin Test

Objective

There are two primary objectives for spin testing. First is to qualify the Gen 1 prototype for operation in a manned area. The second is to confirm analytical and FEA predictions for rotor failure speed.

AFS Trinity, a subcontractor on this project, advised on applying a long-standing principal and practice in establishing the safety criteria. [ref. Bender, *Criteria for Safe Flywheel Operation*, Trinity Flywheel Power whitepaper, May 7, 1997]. In conformance with this practice operation of a flywheel rotor in a manned area must be limited to 70.7% of the speed attained in a spin test in order to assure a factor of safety of 2.0 with respect to tensile stress within the rotor. Therefore, operation at approximately 7,800 RPM requires attaining 11,000 RPM in a spin test.

Other safety requirements include homology between the spin test article and the rotor used in the flywheel system and methods and equipment that snub a 'loose rotor' event.

Method

Spin testing was conducted at Test Devices, Inc., Hudson MA. The test method is summarized here.

A spin test article was supplied to Test Devices. The spin test article comprised a hub and rim built in the same lot as the hub and rim used in the prototype and was wound with the wire from the same procurement and same winding process as used in the prototype. The spin test article did not incorporate a motor.

Test Devices determined that the rotor could be tested as-is and did not require balancing. A quill shaft was installed. A proof test of a single cycle to the intended maximum operating speed of 7,850 RPM was conducted. This was followed by a 6 cycle test between 2,000 RPM and 7,850 RPM. Five cycles had been requested, the sixth cycle was added at the discretion of the test director. The rotor was visually inspected and found to be free of structural defects although some excess epoxy coating had come off. At the outset of the burst test we decided that in the event that the rotor remained intact to 11,000 RPM that we would stop the test at that point and not accelerate the rotor further.

Results

Balance change is the primary indication that the rotor has deformed as a result of spin stresses. The proof test and cycle test resulted in no balance change to the rotor.

The high speed test intended to be a burst test resulted in a small balance shift that occurred at about 9,400 RPM. No further change in balance was observed above this speed.

Upon completion of the run visual inspection indicated no movement or dislocation of the outer layer of wire.

FEA of the spin test rotor suggested that delamination would occur progressively starting around 9,000 RPM. There was no quantitative forecast of the resulting unbalance that would accompany delamination. The freedom from balance change and the lack of evidence from the post-test visual inspection indicate that delamination either did not occur or was benign.

The surface speed attained at 11,000 RPM was 530 m/s. This exceeds all known published values for a cylindrical metal rotor intended for use as a flywheel.

Kinetic energy of the rotor at 11,000 RPM was 10 kWh. This exceeds all known published values for energy stored in a flywheel rotor during a spin test.

The following images are excerpted from the Test Devices report:

Figure 2 – Test Configuration

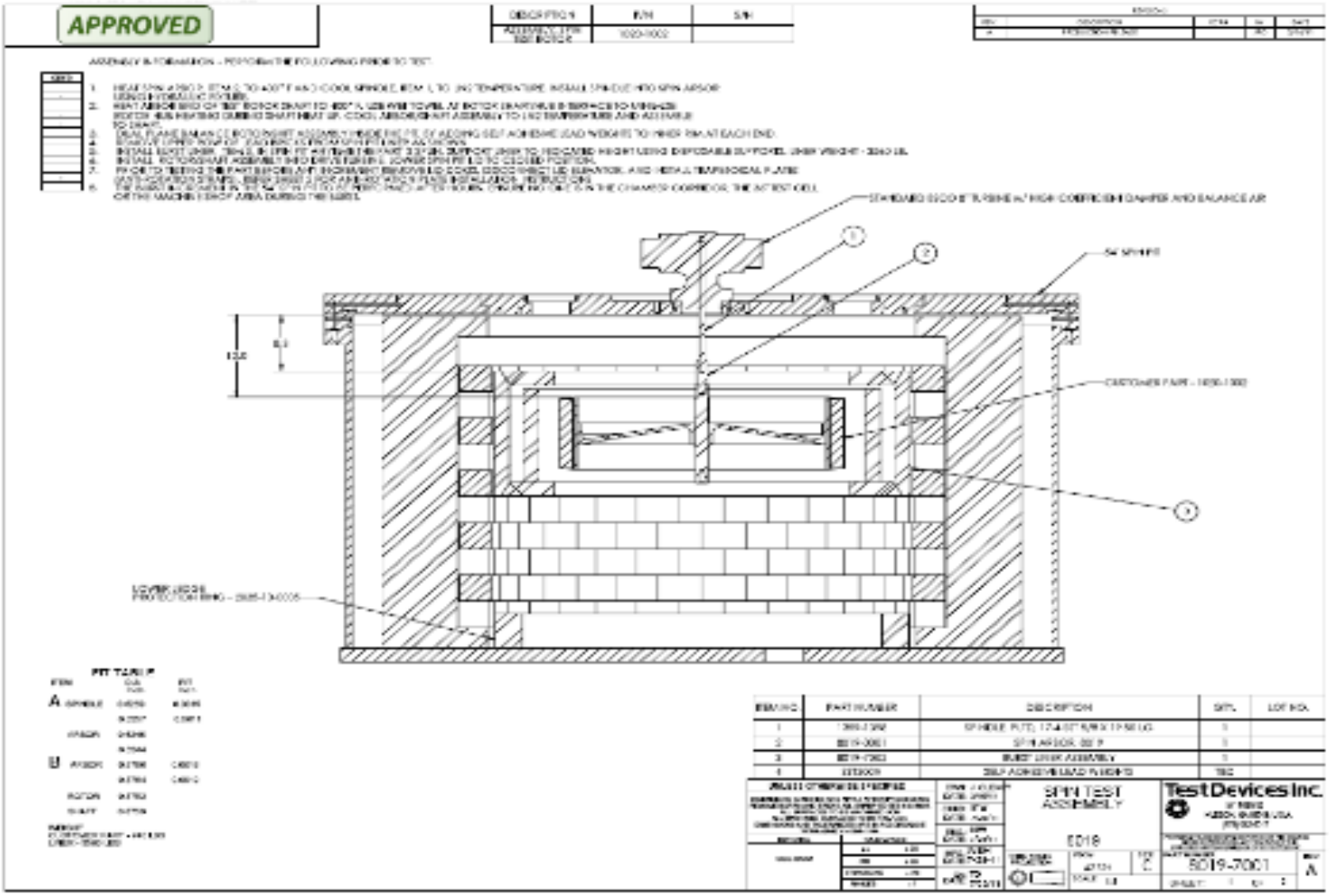

Figure 3– Test Rotor after test to 11,000 RPM

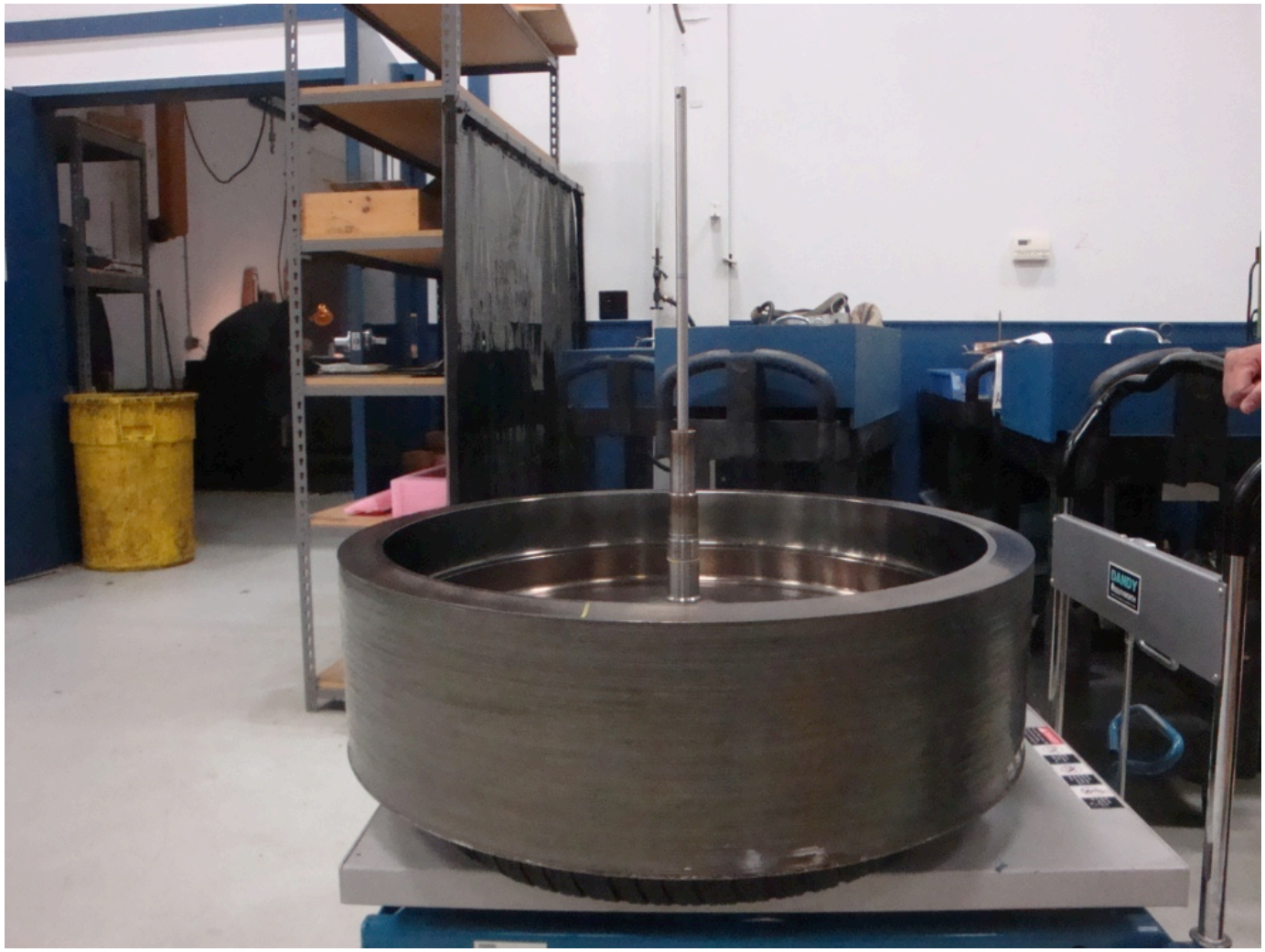

Figure 4 – Cycle Test Data

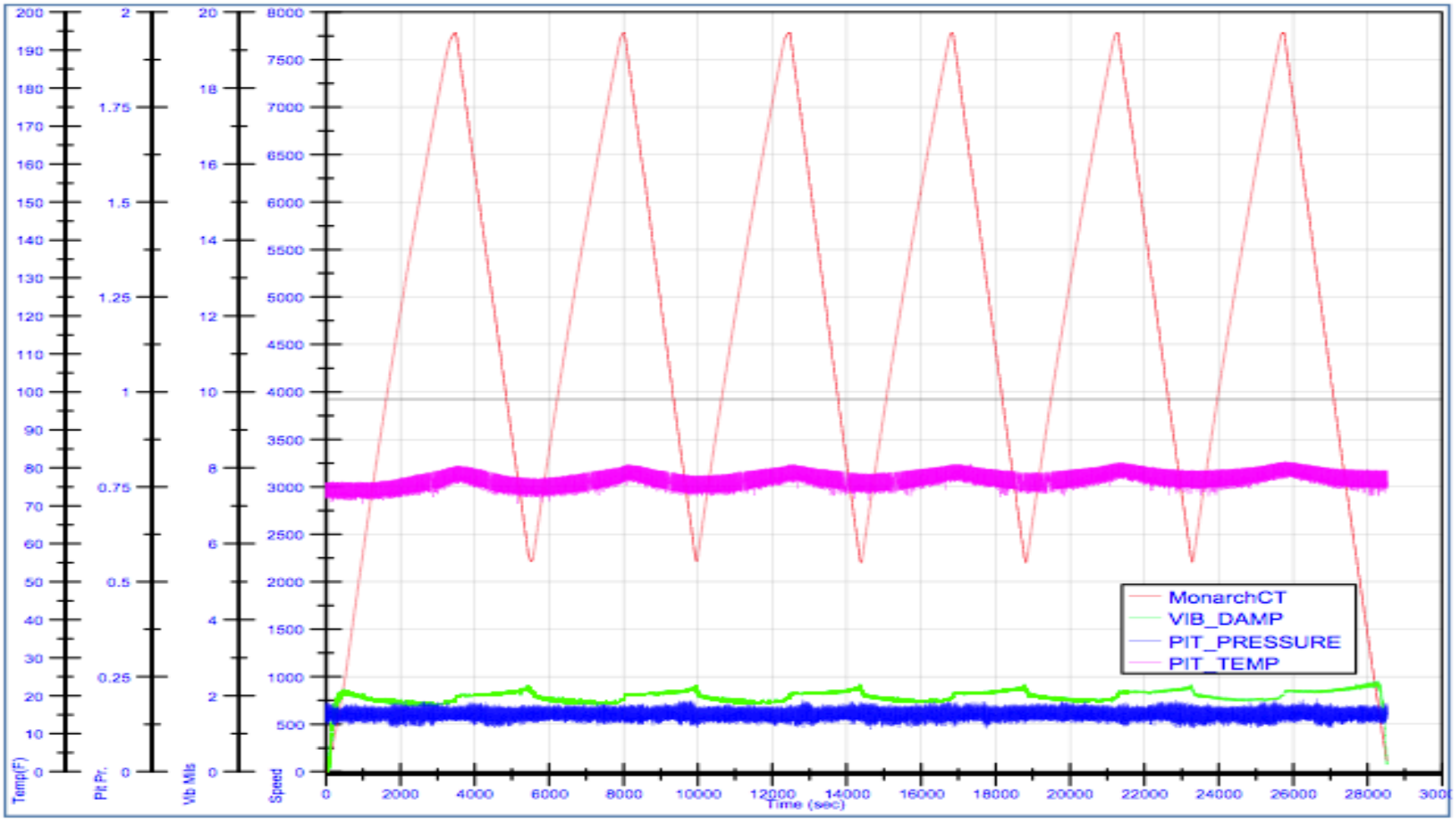

Figure 5 – High Speed

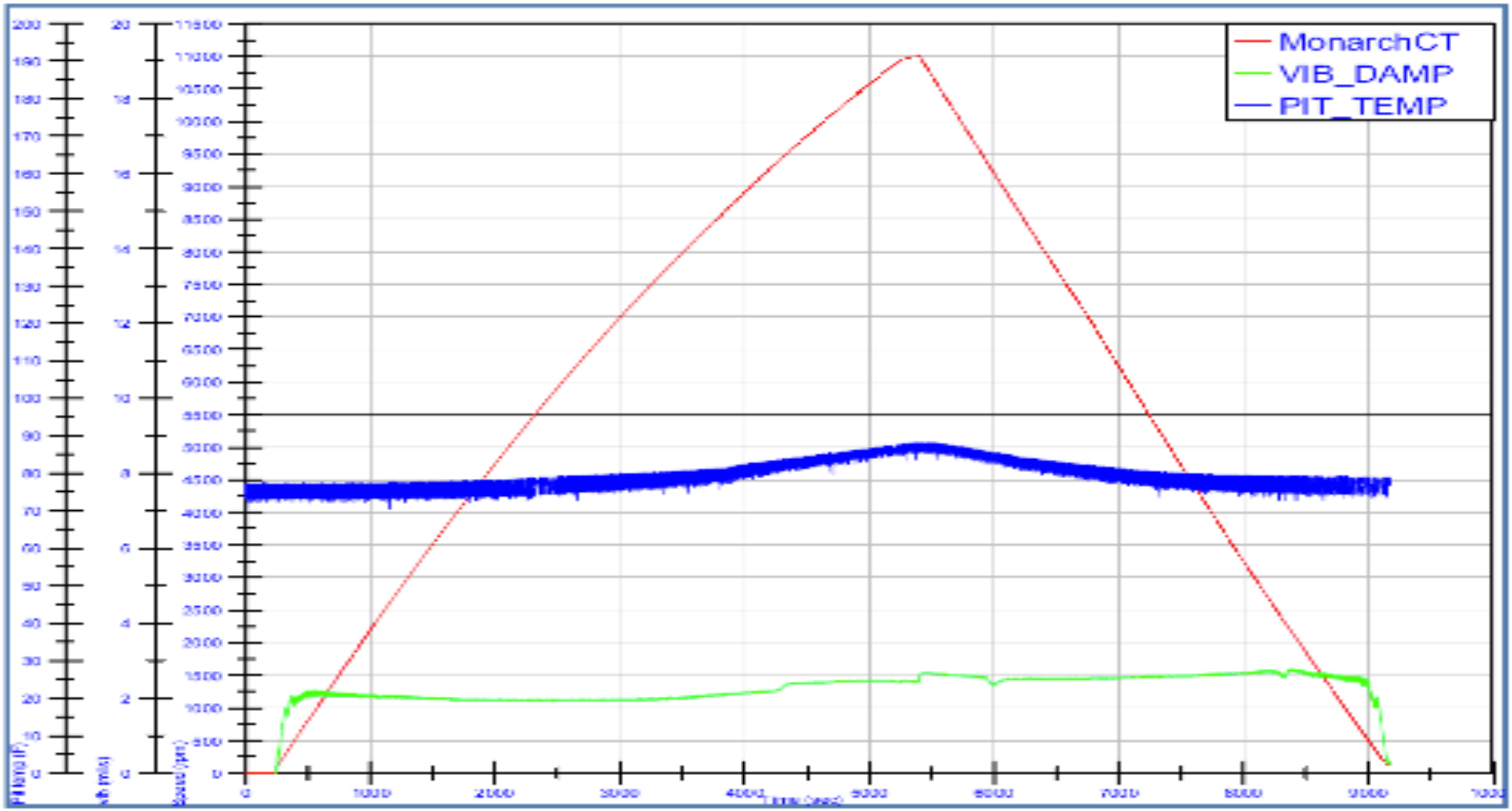

4.4 Operability

Objective

The Objective of Operability testing is to establish safe and reliable operation of the prototype flywheel system up to the operating speed limit.

Method

The flywheel system was operated using the Labview interface. Several modes of operation were conducted:

- Constant current (constant torque) acceleration and deceleration
- Speed control (constant speed)
- Bus voltage regulation
- Coasting
- Deceleration using dump resistor

Under constant current acceleration or deceleration the operator enters a target speed. The system then accelerates or decelerates the rotor to the set speed at constant current.

Under voltage control the operator adds sources or loads to the DC bus. When a source is added, bus voltage rises and the flywheel system absorbs energy in order to regulate bus voltage. When a source is removed or a load is added that pulls bus voltage down, the flywheel system sources energy in order to support bus voltage.

During coasting flywheel leads are disconnected from the power electronics. This mode is used to determine drag loss.

Deceleration using a dump resistor connected directly across the flywheel phase leads is a safety mode intended to decelerate the flywheel in the event of a power electronics failure.

Over the course of operability testing bearing temperature and rotor runout (unbalance) are monitored and recorded.

Results

From August 12, 2011 through October 17, 2011 data were collected from 70 tests. Of these 16 were measurements of vacuum behavior, 9 were measurements of bearing mount properties, and 44 were test runs of the prototype flywheel system.

Throughout operability testing bearing temperature has remained low, the machine has been free from mechanical failure, safety systems and equipment have worked as designed, and vacuum has decreased.

After initial assembly base pressure in the flywheel assembly was around 5000 mtorr. The rotor outgassed over a period of about a month. Eventually base pressure decreased to less than 100

mtorr. Subsequently, pumping after exposing the rotor to atmospheric pressure during maintenance quickly restores the lowest base pressure.

The bearings are passively cooled by conduction to the housing. At no point in the testing did bearing temperature rise more than 15F above ambient.

A number of bearing configurations were tested with the goal of minimizing the coupling of spin energy into whirl modes and suppressing excursion as the rotor traversed a cylindrical resonant mode. As the mount system evolved progressively higher speeds were attained.

4.5 Flywheel Loss Measurement

Objective

The objective of measuring drag loss is to determine the power required to maintain the rotor at a constant state of charge. The forces acting to decelerate the rotor include bearing drag, aerodynamic drag, and eddy current losses due to the interaction between the rotating magnetic field of the motor and stationary conductors including wire and the motor base plate.

Method

Flywheel losses are determined by allowing the flywheel to coast. The deceleration rate is measured and losses are calculated using the design value for rotor moment of inertia. In order to isolate flywheel losses from electrical losses the stator leads are disconnected from the drive. During coasting, the deceleration rate is low and allowing the rotor to coast to rest from the speeds attained in tests to date would take days. Instead, coating measurements were obtained as part of operability testing by allowing the rotor to coast for 30 – 120 minutes at various points in the operability runs. We found that coasting intervals of in this range were long enough to allow a reasonably accurate calculation of deceleration rate.

Results

Coasting losses measured during runs conducted on 9/20/11 and 9/23/11 are presented here. Both coasting loss tests were conducted using the same bearing configuration. Run data for the 9/20/11 test are shown in the time and speed domains. The first plot shows run data in the time domain. The flywheel was accelerated from rest to about 3,225 RPM in steps. Runout and bearing temperature were observed at each step and speed was increased on the basis of these parameters remaining stable. As this run was conducted prior to the high-speed spin test speed was limited to the low end of the operating speed range (40% of maximum operating speed).

Upon reaching the maximum operating speed for the run, the stator leads were disconnected and machine was allowed to coast over a period of 4,259 seconds the rotor decelerated by 138

RPM. The deceleration rate over this interval was 117 RPM per hour and the corresponding coating loss is 63.5W at 3,160 RPM.

The lower plot shows deceleration rate and drag loss in the speed domain.

Figure 6 – Coasting Loss Test

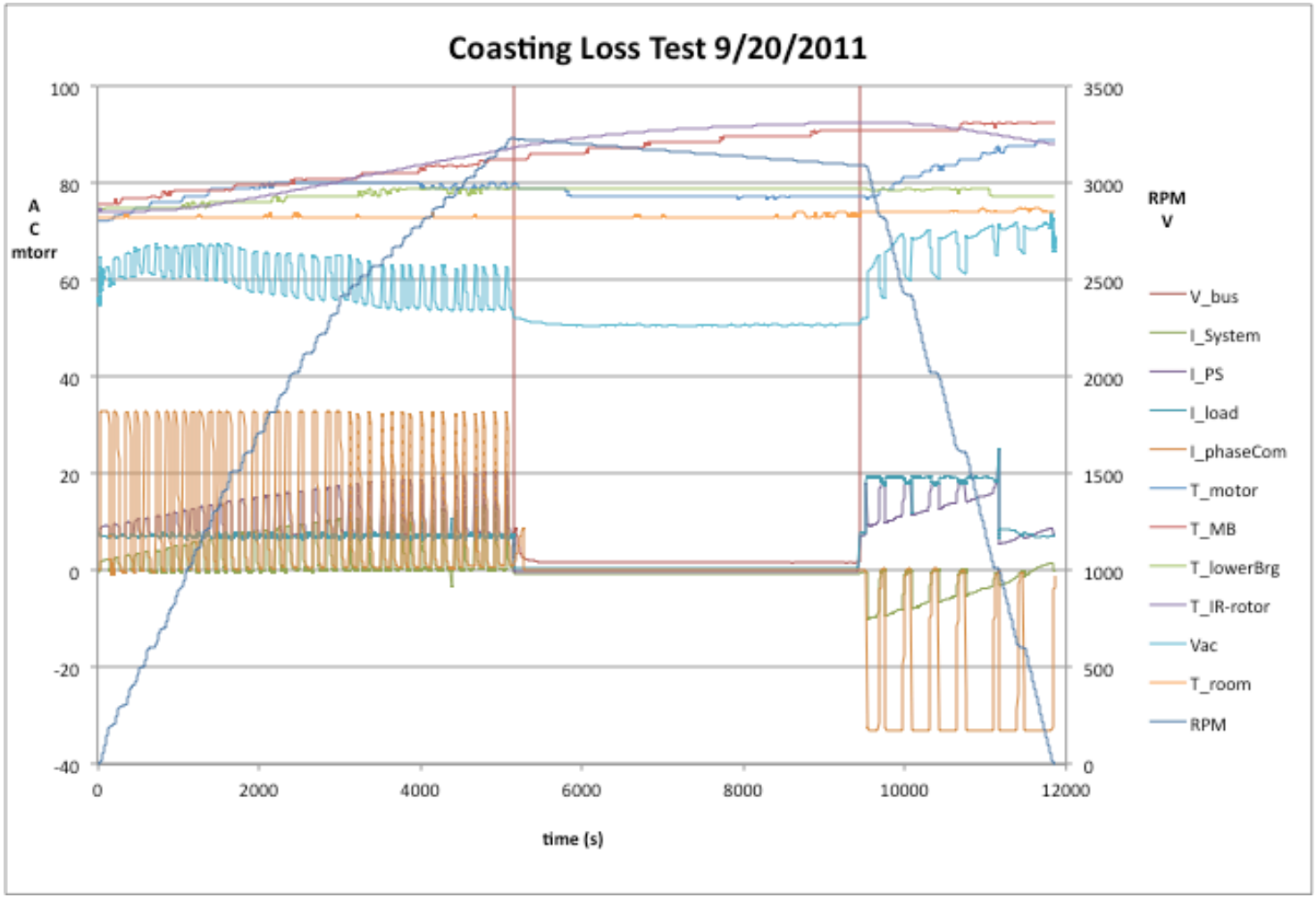

Figure 7 – Calculated Coasting Losses

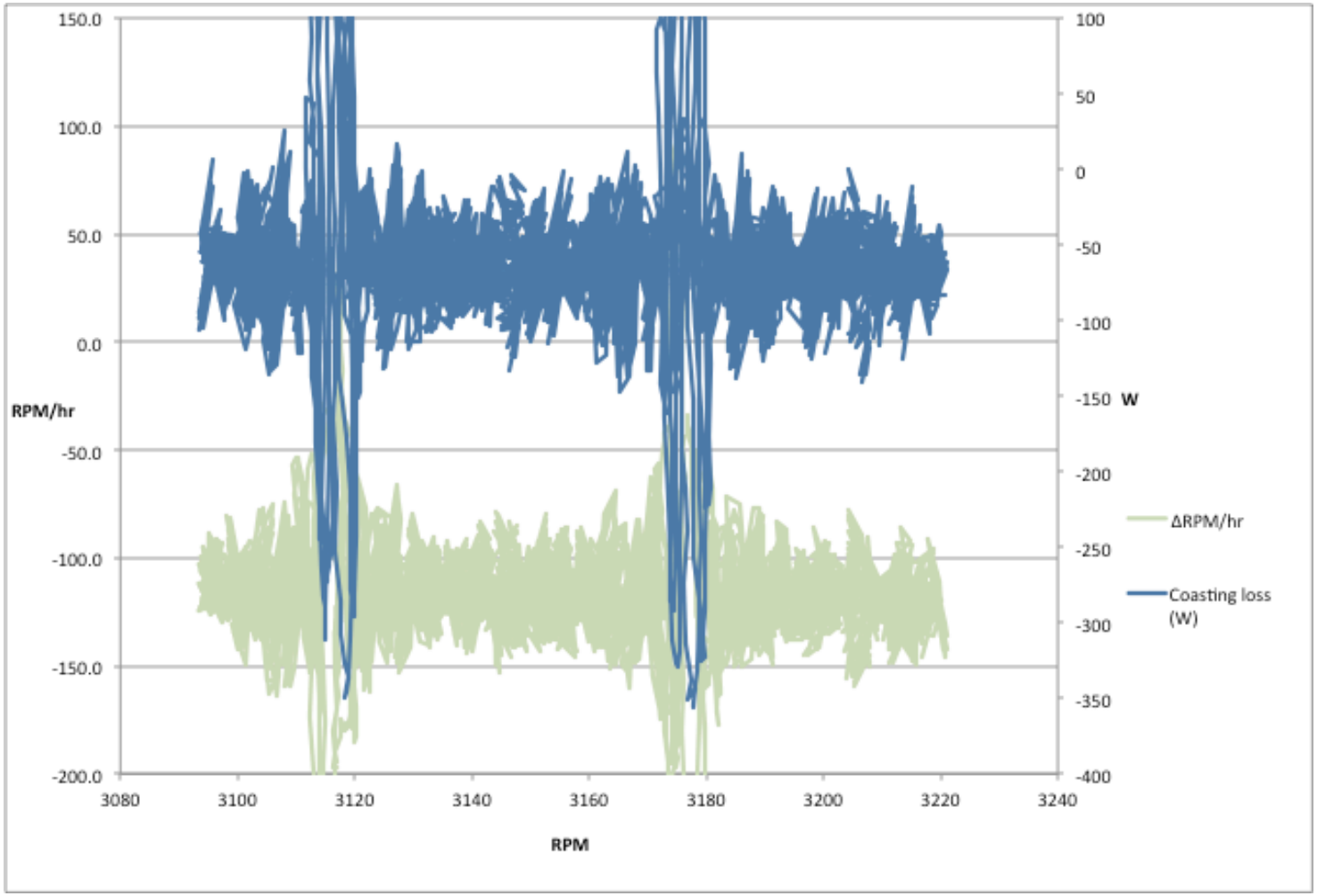

During the coasting loss run conducted on 9/23/11 the rotor was allowed to coast over a period of 7,025 seconds during which speed decreased by 177 RPM from 2,523 RPM to 2,346 RPM. The deceleration rate and coasting loss were 91 RPM per hour and 36 W at 2,440 RPM.

The loss measurements from these two runs are combined below to forecast coasting loss at high speed.

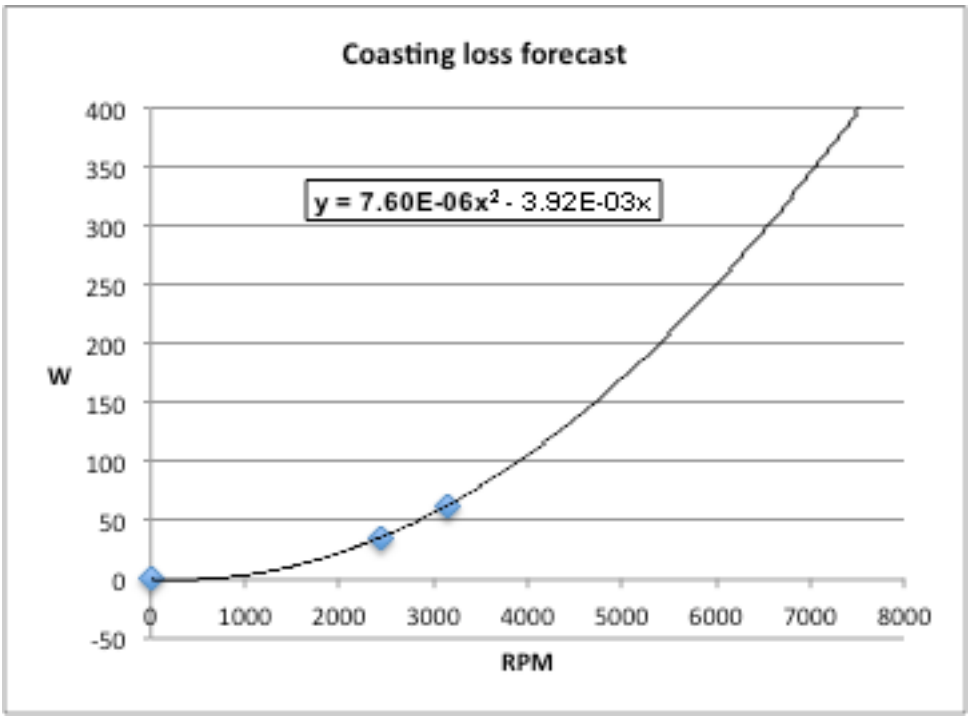

Figure 8 – Coasting Loss Forecast

A constant deceleration rate (RPM per hour) would correspond to a coasting loss that scales with the square of speed. Since deceleration rate was not constant and was found to be higher at higher speed, it appears that losses increase more rapidly than with the square of speed.

If coasting loss varied with the square of speed, loss at full speed would be in the range of 370 W – 390 W. The trend line indicates that loss will exceed 400 W.

4.6 Electrical Machine Performance

Objective

The motor-generator in the Gen 1 was designed to minimize copper losses for maximum efficiency.

Method

Prior to assembly flux in the airgap and resistance of the stator were measured. After assembly, EMF produced at the phase leads was measured. Measurements were compared to the predicted values

Results

The following are comparisons of target and actual values for a variety of parameters.

Table 6 – Target vs. Actual Values

Parameter	Sym	Target Value	Actual Value
Airgap flux (at center of poles)	B	0.35 T	0.325 T (<)
Back EMF Constant (L-L)	Kv	.023 Vrms/rpm	.0213 Vrms/rpm (<)
Phase Resistance	Rp	32 mOhm	37.7 mOhm (>)
Copper Efficiency ** (3460 rpm, 10kW)	η_c	94.7 %	94.1% (<)
Copper Efficiency (7750 rpm, 10kW)	η_c	99.0 %	98.6% (<)

Back EMF is slightly lower than predicted by 7%. This amount of error is acceptable and will yield 7% higher phase currents during operation at any given power.

Phase Resistance is higher by 18% and will reduce the copper efficiency slightly as shown in the table.

** $\eta_c = 1 - (\text{Power} * \text{Rp}) / (\text{Kv} * \text{rpm})^2$

4.7 Ancillary System Losses

Objective

Ancillary systems consume power at a rate that is not dependent on flywheel charge or discharge power and must be accounted for separately.

Method

The auxiliary power consumption of the Gen 1 flywheel energy storage system was measured and recorded. The measurements were conducted under three conditions: when the flywheel was completely powered down, when the flywheel was ramping up to a predefined rotation speed, and when the flywheel was ramping down to a predefined rotation speed. The results of the measurements indicate that the power consumptions are a fraction of the flywheel power capability of 10 kW. When the flywheel is powered down, the total auxiliary power consumption

is 136 W. The auxiliary power consumption is slightly higher when the flywheel is in operation at 141 W.

The first measurement was done when the flywheel was completely powered down. Under this condition the predicted auxiliary power consumption should be lowest. Initially, all the electronic equipment inside the main cabinet were turned on, and the total power consumption was measured. Then one by one, the electronic equipment were powered down, and the power dissipation was measured again. The difference in the power consumption reading between each consecutive reading was calculated to find the power consumption of individual electronic modules.

The second measurement was done when the flywheel was ramping up to a predefined rotation speed (1600 rpm). Since the electronic equipment such as DC Power Supplies, Temperature Sensors, XYZ Position Sensors, Cabinet Fans, and Motor Drive Fan consume the same amount of power regardless of the operational condition of the flywheel, the total power consumption measured in step one can subtracted from the total power consumption measured in this step. The extra power consumption should reflect the power consumed by the motor drive when the flywheel was ramping up to a predefined speed.

Results

Static Power Consumption:

Table 1 shown below contains the measured power consumptions of various electronic modules inside the main cabinet. The first row represents the total power consumption when all the electronic equipment are operating as a single unit, while the rest of the items in the table represent the breakdown of different electronic equipment.

Table 7. Power consumption

Equipment	Real Power Consumption (W)
Everything ON	136
Cabinet Fans (4 total)	50
Motor Drive Fan (1)	28
DC Power Supplies	22
Bearing Drive	3
Motor Drive	12
Bearing Controller Board	3
Supervisory Controller Board	4
XYZ Position Sensors (4)	8
Temperature Sensors (4)	5
Back Up Battery Charging	6

As can be seen in table 1, the cabinet fans consume the most power, while the microcontroller boards and the bearing drive consume the least amount of power.

Ramp Up Power Consumption:
The total real power consumptions measured when the rotation speed is at 340 rpm and when the rotation speed is 1500 rpm are equivalent, which is 141 W. By subtracting the total real power consumption measured in the previous step (136 W) from the total real power consumption measured in this step (141 W), the extra power consumption of the motor drive is calculated, which is 5 W. This is the power required to operate the inverter.

Vacuum Pump Power Consumption:
After have reached a steady-state vacuum, the vacuum pump was found to consume approximately 325 Watts in continuous operation. This number should not be added to the 136 Watts of auxiliary power because in a realistic application, the vacuum pump should be cycled off, and back on once the flywheel containment pressure rises above a maximum allowed vacuum pressure. The duty cycle of this cycling will vary depending on the leak rate. A reasonable duty cycle might be about 10%; that would bring the average pumping power down to 33 Watts.

Conclusion
As the results indicate, the auxiliary power consumption is a small fraction of the maximum flywheel power capability at full speed. (136 + 33)/10000 = 1.7%

5. Grid Impacts and Benefits

Grid impacts and benefits were not applicable in Phase 1 of this program.

6. Major Findings and Conclusions

Major technical findings and conclusions are as follows:

(1) High strength steel wire was confirmed to be a suitable material for low-cost flywheel rotors. The material, with greater than 350,000 psi tensile strength, was purchased in low quantities (thousands of lbs) at less than 5% of the cost / lb of carbon fiber. The material performed above expectations in spin testing, with over 150,000 stress cycles using accelerated testing procedures, and Phase 1 of this program established a credible path toward significantly lower cost flywheel rotors constructed from high strength steel wire.

(2) Low-cost manufacturing techniques of flywheel rotors using high-strength steel wire was confirmed. Manufacturing of two flywheel rotors was completed in Northern California using standard winding equipment and low-cost processes.

(3) Balance of system costs (bearings, motor, vacuum vessel, power electronics) make up the majority of the cost of an anticipated commercial system. While the cost advantages of using steel wire are clearly attractive, Amber Kinetics has identified the need to either scale up internal staff or work with an industrial partner to develop more detailed manufacturing cost estimates for a grid-connected flywheel energy storage system.

Lessons learned during Phase 1 of the program were the following:

(1) Vendor risk management. A qualified secondary spin test facility would have greatly reduced schedule risk to the program. The selected spin test facility experienced an unexpected 10-month delay in spin test scheduling for our flywheel rotor. The delay had nothing to do with Amber's flywheel rotor configuration. The issue was with a previous customer part, which had caused damage and delay to the spin pit. The schedule for the Amber Kinetics flywheel development program was not negatively impacted by this delay due to the required initial low-speed testing period that was still underway when the over-speed spin test was finally scheduled.

(2) Manufacturing costs for complete flywheel systems are dominated by balance-of-system costs. In this program, the Amber Kinetics flywheel rotor achieved an estimated > 10x cost reduction vs. current start-of-the-art flywheel rotors in commercial operation. However, the rotor cost was a fraction of the overall bill of material cost of the flywheel system. Significant costs in the vacuum vessel and sensors were incurred. Phase 1 in the program determined that scaling up to larger, commercial-scale designs is technically achievable and imperative to achieving low capital costs.

7. Future Plans

The next step is to execute Phase 2 to complete commercial trade studies and a detailed design of the Gen2 commercial-scale flywheel system. Amber Kinetics plans to develop this demonstration system in collaboration with a commercial partner and is in ongoing discussions for additional cost-share to complete this program.

In Phase 3, this program aims to activate and test one or more flywheel systems and connect the systems to the utility grid for Metrics and Benefits data collection and reporting.

Appendix A: List of Acronyms

A	Ampere
AC	Alternating current
CAN	Control area network
DAQ	Data acquisition system
DC	Direct current
DOE	Department of energy
EMF	Electromagnetic field
F	Fahrenheit
FEA	Finite element analysis
kWh	Kilowatt hour
mtorr	Millitorr
mV	Millivolt
PSI	Pounds per square inch
RPM	Rotations per minute
RTD	Resistance temperature detector
uF	Microfarad
USB	Universal serial bus
UUT	Unit under test
V	Volt
VAC	Alternating current voltage
VDC	Direct current voltage
W	Watt